

# A simplified framework for fast and reliable measurement of leaf turgor loss point

Francesco Petruzzellis<sup>1\*</sup>, Tadeja Savi<sup>2</sup>, Giovanni Bacaro<sup>1</sup>, Andrea Nardini<sup>1</sup>

<sup>1</sup>Dipartimento di Scienze della Vita, Università degli Studi di Trieste, via L. Giorgieri  
10, 34127, Trieste, Italia

<sup>2</sup>University of Natural Resources and Life Sciences, Vienna, Department of Crop  
Sciences, Division of Viticulture and Pomology, Konrad Lorenz Straße 24, A-3430  
Tulln, Austria

\*Corresponding author: [fpetruzzellis@units.it](mailto:fpetruzzellis@units.it)

## HIGHLIGHTS:

- Leaf turgor loss point ( $\Psi_{\text{tlp}}$ ) defines drought tolerance of plant species.
- $\Psi_{\text{tlp}}$  could be estimated from the osmotic potential at full turgor ( $\pi_0$ ).
- $\pi_0$  could be easily measured with a dewpoint hygrometer.
- Accounting for leaf dry matter content improves estimates of  $\Psi_{\text{tlp}}$  from  $\pi_0$ .

22 ABSTRACT:

23 Drought tolerance shapes the distribution of plant species, and it is mainly  
24 determined by the osmotic potential at full turgor ( $\pi_0$ ) and the water potential at turgor  
25 loss point ( $\Psi_{\text{tlp}}$ ). We provide a simplified framework for  $\pi_0$  and  $\Psi_{\text{tlp}}$  measurements  
26 based on osmometer determination of  $\pi_0$  ( $\pi_{0\_osm}$ ). Specifically, we ran regression  
27 models to i) improve the predictive power of the estimation of  $\pi_0$  from  $\pi_{0\_osm}$  and  
28 morpho-anatomical traits; ii) obtain the most accurate model to predict  $\Psi_{\text{tlp}}$  on the  
29 basis of the global relationship between  $\pi_0$  and  $\Psi_{\text{tlp}}$ . The inclusion of the leaf dry  
30 matter content (LDMC), an easy-to-measure trait, in the regression model improved  
31 the predictive power of the estimation of  $\pi_0$  from  $\pi_{0\_osm}$ . When  $\pi_{0\_osm}$  was used as a  
32 simple predictor of  $\Psi_{\text{tlp}}$ , discrepancies arose in comparison with global relationship  
33 between  $\pi_0$  and  $\Psi_{\text{tlp}}$ .  $\Psi_{\text{tlp}}$  values calculated as a function of the  $\pi_0$  derived from  $\pi_{0\_osm}$   
34 and LDMC ( $\pi_{0\_fit}$ ) were consistent with the global relationship between  $\pi_0$  and  $\Psi_{\text{tlp}}$ .  
35 The simplified framework provided here could encourage the inclusion of  
36 mechanistically sound drought tolerance traits in ecological studies.

38 KEYWORDS:

39 dewpoint hygrometer; mechanistic traits; osmotic potential; water availability; water  
40 potential

## 1. INTRODUCTION

Plant functional traits are defined as morphological, physiological, or phenological features measurable at the individual level, from the cell to the whole-organism (Violle et al., 2007). Recently, Brodribb (2017) suggested to distinguish “mechanistic” traits, which comprehends plant’s features clearly associated to a physiological process, from general functional traits (such as leaf mass per unit area), which rather represent “syndromes” that could be driven by several different physiological functions and associated trade-offs. Mechanistic traits have been increasingly included in trait-based studies and provided novel insights into several ecological processes, ranging from species assembly rules (Blackman et al., 2012; Brodribb et al., 2014), invasion of alien plant species (Petruzzellis et al., 2018), and vegetation dynamics under ongoing climate changes (Anderegg, 2015). As an example, hydraulic traits (e.g.  $\Psi_{50}$ , the water potential inducing 50% loss of hydraulic conductivity, or  $K_s$ , the stem specific hydraulic conductivity) have been used to model plant species distribution (Costa-Saura et al., 2016; Larter et al., 2017), and they were shown to correlate with growth rate and risk of mortality under drought (Anderegg et al., 2015; Choat et al., 2012; Fan et al., 2012).

Leaf water relation parameters have been recently proposed as predictors of the position of a species along the “fast-slow” whole plant economic spectrum (Blackman, 2018; Zhu et al., 2018), as they correlate to both leaf hydraulic and economic traits (Nardini and Luglio, 2014; Trifiló et al., 2016). Specifically, leaf osmotic potential at full turgor ( $\pi_0$ ) and the leaf water potential at turgor loss point ( $\Psi_{tlp}$ ) are strongly linked to species-specific ability to tolerate leaf dehydration (Bartlett et al., 2012b) and consequently to sustain stomatal conductance, photosynthesis and growth even under water shortage conditions (Bartlett et al., 2016; Tognetti et al., 2000). In particular,  $\Psi_{tlp}$  indicates the water potential inducing loss of cell turgor pressure (Bartlett et al., 2012b), which is critical to maintain gas exchange and growth (Brodribb et al. 2003). In their recent analysis, Zhu et al. (2018) have reported that  $\Psi_{tlp}$  is correlated with leaf carbon investment, as species with lower  $\Psi_{tlp}$  tend to have higher leaf density ( $d_{leaf}$ ) and leaf mass per unit area (LMA). Turgor loss point also correlates with habitat moisture, as species living in arid environments usually have lower values of  $\Psi_{tlp}$  than species living under higher water availability (Bartlett et al., 2012b; Lenz et al., 2006; Zhu et al., 2018). Given the correlation between  $\Psi_{tlp}$ ,

75 hydraulic and economic traits and environmental features, the inclusion of the turgor  
76 loss point in ecological studies holds promises to provide important insights on  
77 ecological and evolutionary patterns in plants.

78  $\Psi_{\text{tlp}}$  has been traditionally estimated from water potential isotherms (or pv-  
79 curves, Tyree and Hammel 1972), i.e. by measuring the progressive decrease of the  
80 water potential and of the water content during leaf dehydration. This procedure is  
81 time-consuming, and this probably limited the inclusion of  $\Psi_{\text{tlp}}$  in studies involving  
82 large numbers of species/individuals and/or study sites. Recently, Bartlett et al.  
83 (2012b) have reported that the variation of  $\Psi_{\text{tlp}}$  both between and within species is  
84 mainly driven by changes in  $\pi_0$ , which reflects solutes concentration in cells at full  
85 turgor. These two traits resulted highly correlated to each other, as species with  
86 lower  $\Psi_{\text{tlp}}$  also have lower values of  $\pi_0$  (Bartlett et al., 2012b). Consequently, both  
87 traits could be considered as useful parameters to predict species drought tolerance,  
88 and  $\pi_0$  could be used as a proxy of turgor loss point. Alternative methods have been  
89 proposed to obtain  $\pi_0$ , e.g. by directly measuring the osmotic potential of sap  
90 extracted from leaf tissues using a thermocouple psychrometer. In particular, rapid  
91 freeze and thaw of leaf samples, that induces cell disruption and the release of  
92 symplastic contents, is considered the most accurate procedure to measure  $\pi_0$  with  
93 an osmometer ( $\pi_{0\_osm}$ ). Recently, Bartlett et al. (2012a) proposed a framework to  
94 predict both  $\pi_{0\_pv}$  (osmotic potential at full turgor derived from pv-curves) and  $\Psi_{\text{tlp}}$   
95 from  $\pi_{0\_osm}$  measurements. In their analysis, the authors tested various models  
96 including different morpho-anatomical leaf traits, and they reported that models  
97 including bulk modulus of elasticity ( $\epsilon$ ) and  $d_{\text{leaf}}$  significantly improved the ability to  
98 predict  $\pi_{0\_pv}$  from  $\pi_{0\_osm}$  measurements. However,  $\epsilon$  is generally derived from pv-  
99 curves, so that including this parameter in the derivation of  $\pi_{0\_pv}$  does not represent a  
100 major advantage. Also,  $d_{\text{leaf}}$  measurements can be laborious and prone to errors as  
101 far as volume estimates are concerned. Hence, a simplified framework for estimation  
102 of  $\pi_0$  would be useful for ecological studies.

103 In this study, we measured several functional traits as well as water relation  
104 parameters derived from pv-curves in 27 species, with the aim to provide a simple  
105 framework to estimate  $\pi_{0\_pv}$  and  $\Psi_{\text{tlp}}$  from measurements of  $\pi_{0\_osm}$  obtained with a  
106 dewpoint hygrometer. The specific aims were to i) obtain a model to predict  $\pi_{0\_pv}$  on  
107 the basis of  $\pi_{0\_osm}$  and easy-to-measure functional traits (like LMA or leaf dry matter

108 content); ii) obtain the most accurate model to predict  $\Psi_{\text{tip}}$  on the basis of the global  
109 relationship between  $\pi_0$  and  $\Psi_{\text{tip}}$ .

## 110 111 2. MATERIALS AND METHODS

### 112 113 *2.1 Leaf traits measurements*

114 To model the estimation of the osmotic potential at full turgor ( $\pi_0$ ) and of the water  
115 potential at turgor loss point ( $\Psi_{\text{tip}}$ ) from  $\pi_0$  values obtained with a dewpoint  
116 hygrometer ( $\pi_{0\_osm}$ ; see below), we selected 27 temperate and Mediterranean woody  
117 species (Table S1) with different levels of drought resistance. Species were sampled  
118 in natural habitats in the Karst region (NE Italy), or in the Botanical Garden of  
119 University of Trieste. Additional data were obtained from previous studies performed  
120 in our laboratory (see Table S1 for references).

121 Three leaves were sampled from different individuals of each species to  
122 measure  $\pi_{0\_osm}$ . Twigs were detached from branches and were rehydrated overnight.  
123 One leaf per twig was roughly crumpled up and sealed in cling film. Then, it was  
124 immersed in liquid nitrogen ( $\text{LN}_2$ ) for 2 min. The leaf (still sealed in cling film) was  
125 then carefully ground and stored in sealed plastic bottles at  $-20^\circ\text{C}$ . Before  
126 measurements, samples were thawed at room temperature for 5 min while still  
127 sealed in cling film and in plastic bottles, to avoid evaporation effect on  
128 measurements (Bartlett et al., 2012a). Finally,  $\pi_{0\_osm}$  was measured with a dewpoint  
129 hygrometer (Model WP4, Decagon Devices Inc., Pullman, Washington, USA).

130 Water potential isotherms (pv-curves) were measured to obtain reference  
131 values for  $\Psi_{\text{tip}}$  and  $\pi_{0\_pv}$ . Fresh leaves were rehydrated for 12 h with their petioles  
132 immersed in pure water and pv-curves were measured using the bench dehydration  
133 technique, by repeatedly measuring water loss and water potential with a balance  
134 and a pressure chamber (model 1505D, PMS Instruments, Albany, OR, USA),  
135 respectively, during progressive sample dehydration. Water potential ( $\Psi_{\text{leaf}}$ ) and  
136 cumulative weight loss (WI) of leaves were measured until the relationship between  
137  $1/\Psi$  and WI became strictly linear, indicating the loss of cell turgor. Pv-curves were  
138 then elaborated according to Salleo (1983) to calculate the osmotic potential at full  
139 turgor ( $\pi_{0\_pv}$ ), the water potential at turgor loss point ( $\Psi_{\text{tip\_pv}}$ ) and the modulus of  
140 elasticity ( $\epsilon$ ).

141 For each species, leaf morpho-anatomical parameters were measured on 6  
142 leaves from the same individuals sampled for the measurements of  $\pi_{0\_osm}$  and pv-  
143 curves. Specifically, we measured leaf thickness (Th,  $\mu\text{m}$ ), leaf dry matter content  
144 (LDMC,  $\text{mg g}^{-1}$ ), leaf mass per unit area (LMA,  $\text{mg cm}^{-2}$ ) and leaf density ( $d_{\text{leaf}}$ ,  $\text{g cm}^{-3}$ ).

146 Th was measured after rehydrating leaves for 3h using a digital calliper on  
147 three portions of the leaf (top, middle, bottom). Values were then averaged for each  
148 leaf.

149 LDMC and LMA were calculated as:

$$150 \text{ LDMC} = \text{Leaf dry weight} / \text{Leaf turgid weight} \quad (\text{eqn 1})$$

$$151 \text{ LMA} = \text{Leaf dry weight} / \text{Leaf area} \quad (\text{eqn 2})$$

152 Fresh leaves were first rehydrated for 3h and leaf turgid weight was measured with  
153 an analytical balance. Leaves were scanned and leaf area was measured using the  
154 software Image J (Schneider et al., 2012). Leaves were finally oven-dried for 48 h at  
155 72°C and leaf dry weight was measured.

156  $d_{\text{leaf}}$  was calculated as:

$$157 d_{\text{leaf}} = \text{Leaf dry weight} / \text{Leaf fresh volume} \quad (\text{eqn 3})$$

158 Leaf fresh volume was measured using a water displacement method (Hughes  
159 2005), while leaf dry weight was measured as described above.

## 161 2.2 Statistical analysis

162 The first aim of this study was to find an easy and fast method to measure the leaf  
163 osmotic potential at full turgor, based on the work of Bartlett et al. (2012a). To  
164 improve the predictive power of the estimation of  $\pi_{0\_pv}$  from  $\pi_{0\_osm}$  measurements,  
165 we ran a multiple linear regression model to predict  $\pi_{0\_pv}$  (response variable) as a  
166 function of  $\pi_{0\_osm}$  and the leaf traits described above. A Minimum Adequate Model  
167 (MAM) was obtained using package “glmulti” (Calcagno 2013) via minimization of the  
168 corrected Akaike informative criterion (AICc) plus a backward procedure to avoid  
169 multicollinearity among selected explanatory variables. To compare results obtained  
170 by Bartlett et al. (2012a), we evaluated two other linear regression models, setting  
171  $\pi_{0\_pv}$  as the response variable. In a first model, only  $\pi_{0\_osm}$  was set as the predictive  
172 variable, while in the second we considered both  $\pi_{0\_osm}$  and  $d_{\text{leaf}}$  as predictive  
173 variables. Models were then compared on the basis of their predictive power

174 (adjusted  $R^2$ ,  $R^2_{adj}$ ) and, in order to take in account the number of predictors included  
175 in the model, the AICc and their mean absolute error (MAE).

176 The second aim of this study was to test the ability to predict  $\Psi_{\text{tip}_{\text{pv}}}$  both from  
177  $\pi_{0_{\text{osm}}}$  measurements and the fitted values of the MAM ( $\pi_{0_{\text{fit}}}$ ) and compare models'  
178 output with the global relationship between  $\Psi_{\text{tip}}$  and  $\pi_0$  described in Bartlett et al.  
179 (2012b). We first fitted two separated simple linear regression models on the data  
180 measured in the present study, considering  $\Psi_{\text{tip}_{\text{pv}}}$  (response variable) as a function  
181 of  $\pi_{0_{\text{osm}}}$  or  $\pi_{0_{\text{fit}}}$ , respectively. For each model, we calculated coefficient estimates  
182 and associated 95% confidence intervals (95% C.I.),  $R^2_{adj}$ , AICc and MAE.

183 Because the number of species analysed in Bartlett et al. (2012b) differed  
184 from the present study (248 and 27 respectively), we set up a bootstrap procedure  
185 (999 replicates) to obtain comparable values of estimated coefficients.  $\pi_0$  and  $\Psi_{\text{tip}}$   
186 values of 27 randomly selected species from the dataset in Bartlett et al. (2012b)  
187 were chosen. From this selection, we fitted a simple linear regression model  
188 calculating coefficient estimates, 95% C.I.,  $R^2_{adj}$ , AICc and MAE. At the end of this  
189 bootstrap procedure, averaged values were calculated. Differences between  $\Psi_{\text{tip}_{\text{pv}}}$   
190 prediction from  $\pi_{0_{\text{osm}}}$ ,  $\pi_{0_{\text{fit}}}$  and the one derived from Bartlett et al. (2012b) were  
191 determined comparing 95% C.I. of the coefficient estimates and AICc. Specifically,  
192 predictions were assumed to differ if 95% C.I. of coefficient estimates did not overlap  
193 and if the difference between AICc values were  $> 2$  (Burnham and Anderson, 2004).  
194 All statistical analyses were performed using R 3.4.1 (R Foundation for Statistical  
195 Computing, Vienna, AT).

### 3. RESULTS

196  
197  
200 Species scientific name, abbreviation, and associated mean values of leaf traits are  
201 summarized in Tab. S1. Species that sustained higher leaf construction costs (higher  
202 LMA, LDMC and Th) also had higher drought resistance (lower  $\Psi_{\text{tip}_{\text{pv}}}$ ), as shown by  
203 correlation analysis reported in Tab. S2.

204 Although  $\pi_{0_{\text{osm}}}$  resulted a significant predictor  $\pi_{0_{\text{pv}}}$  (Tab. 1), it  
205 underestimated  $\pi_{0_{\text{pv}}}$  at less negative values and overestimated it at more negative  
206 values (Fig. 1). The best model to predict  $\pi_{0_{\text{pv}}}$  included  $\pi_{0_{\text{osm}}}$  and LDMC as  
207 predictive variables (Tab. 1). The inclusion of LDMC significantly improved the

208 predictive power of the model, as the  $R^2_{adj}$  was higher and AICc were lower than  
 209 those calculated on the model including only  $\pi_{0\_osm}$  or the one including both  $\pi_{0\_osm}$   
 210 and  $\epsilon$  (Tab. 1).

**Tab. 1** Summary of the models predicting the osmotic potential at full turgor  
 measured through pv-curves ( $\pi_{0\_pv}$ ) from osmotic potential at full turgor obtained with  
 a dewpoint hygrometer ( $\pi_{0\_osm}$ ) alone, including leaf dry matter content (LDMC) or  
 the modulus of elasticity of cell walls ( $\epsilon$ ).  $R^2_{adj}$  = adjusted  $r^2$ . AICc = Akaike  
 informative criterion corrected for low number of observations. MAE = mean absolute  
 error of the model

$\pi_{0\_pv}$ estimation	Estimate	Std. error	p-value	$R^2_{adj}$	AICc	MAE
<b><math>\beta * \pi_{0\_osm} + \text{intercept}</math></b>				0.46	17.8	0.18
$\beta$	0.681	0.143	<0.001			
intercept	-0.434	0.240	0.08			
<b><math>\beta * \pi_{0\_osm} + \beta_1 * \text{LDMC} + \text{intercept}</math></b>				0.58	11.4	0.12
$\beta$	0.506	0.138	0.001			
$\beta_1$	-0.002	0.001	0.007			
intercept	0.013	0.258	0.96			
<b><math>\beta * \pi_{0\_osm} + \beta_1 * \epsilon + \text{intercept}</math></b>				0.53	16.1	0.17
$\beta$	0.654	0.226	0.17			
$\beta_1$	-0.013	0.132	<0.001			
intercept	-0.319	0.006	0.03			



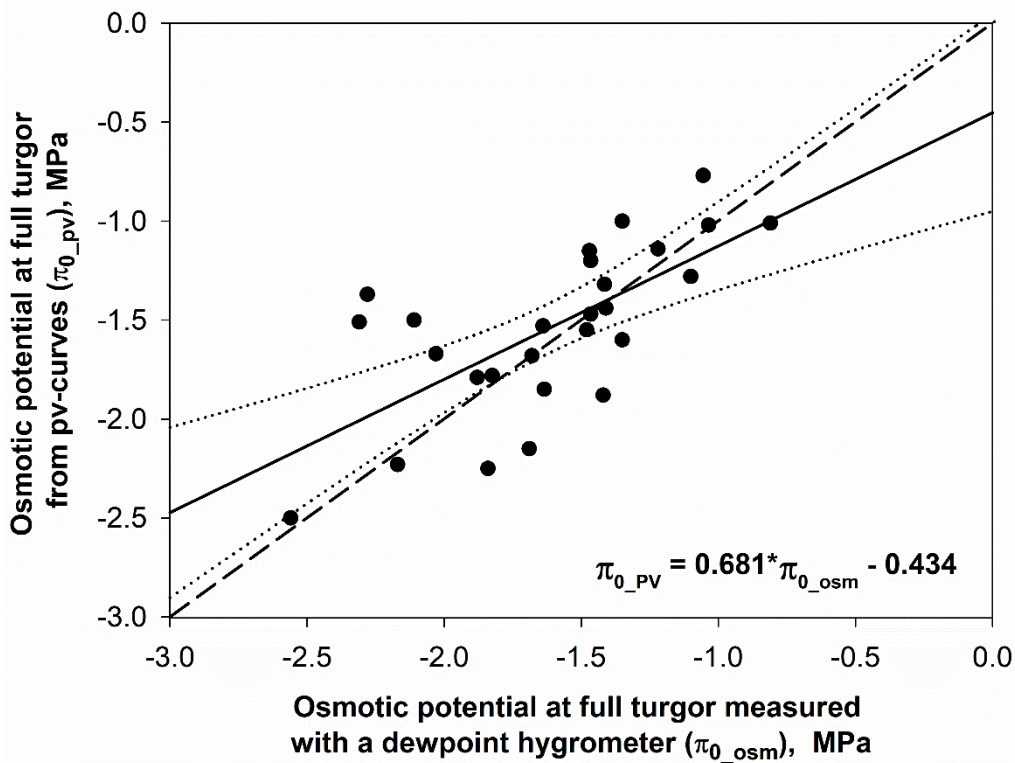


**Fig. 1** Relationship between osmotic potential at full turgor measured with a dewpoint hygrometer ( $\pi_{0\_osm}$ ) and osmotic potential at full turgor measured through pv-curves ( $\pi_{0\_pv}$ ). Dotted lines represent confidence intervals of the regression line (solid line). Dashed line represents the 1:1 line

$\pi_{0\_osm}$  and  $\pi_{0\_fit}$  were tested as predictors of  $\Psi_{t_{lp\_pv}}$ . The parameters of the two derived models were compared with those derived from the relationship between  $\Psi_{t_{lp\_pv}}$  and  $\pi_{0\_pv}$  reported in Bartlett et al. (2012b) and from the iterative procedure described above. The average  $\beta$  and intercept estimates calculated on a reduced number of species were not statistically different from those calculated including the whole dataset provided by Bartlett et al. (2012b) and on the models including  $\pi_{0\_osm}$  and  $\pi_{0\_fit}$  as predictive variables, as 95% C.I. overlapped each other (Tab. 2). However, the model including  $\pi_{0\_fit}$  had higher predictive ability than the one including  $\pi_{0\_osm}$  (Tab.1), as the  $R^2_{adj}$  was higher and AICc and MAE were lower (Tab. 2). In addition, the model including  $\pi_{0\_osm}$  led to overestimation of  $\Psi_{t_{lp\_pv}}$  for values < -2 MPa. As shown in Fig. 2 and Fig. 3, mean values of slope ( $\beta$ ) and intercept

243 calculated on the model including  $\pi_{0\_fit}$  as predictive variable were much closer to  
 244 those calculated on 27 randomly selected species from Bartlett et al. (2012b).

245  
 246 **Tab. 2** Summary of the models predicting the water potential at turgor loss point  
 247 measured through pv-curves ( $\Psi_{tlp\_pv}$ ) from osmotic potential at full turgor obtained  
 248 with a dewpoint hygrometer ( $\pi_{0\_osm}$ ) alone, fitted values of the MAM ( $\pi_{0\_fit}$ ) and from  
 249  $\pi_0$  values provided by Bartlett et al. (2012b). 2.5% and 97.5% represent 95%  
 250 confidence interval limits.  $R^2_{adj}$  = adjusted  $R^2$ . AICc = Akaike informative criterion  
 251 corrected for low number of observations. MAE = mean absolute error of the model.

$\Psi_{tlp\_pv}$ estimation	Estimate	2.5%	97.5%	$R^2_{adj}$	AICc	MAE
<b><math>\beta * \pi_{0\_osm} + \text{intercept}</math></b>				0.47	31.4	0.31
$\beta$	0.899	0.530	1.268			
intercept	-0.581	-1.197	0.034			
<b><math>\beta * \pi_{0\_fit} + \text{intercept}</math></b>				0.61	23.9	0.25
$\beta$	1.313	0.902	1.725			
intercept	-0.032	-0.673	0.609			
<b><math>\beta * \pi_{0\_pv} + \text{intercept}</math> (27 species)</b>				0.87	6.82	0.18
$\beta$	1.211	1.027	1.394			
intercept	-0.057	-0.391	0.276			
<b><math>\beta * \pi_{0\_pv} + \text{intercept}</math> (Bartlett et al., 2012b)</b>				0.87	50.1	0.18
$\beta$	1.205	1.146	1.263			
intercept	-0.062	-0.170	0.044			

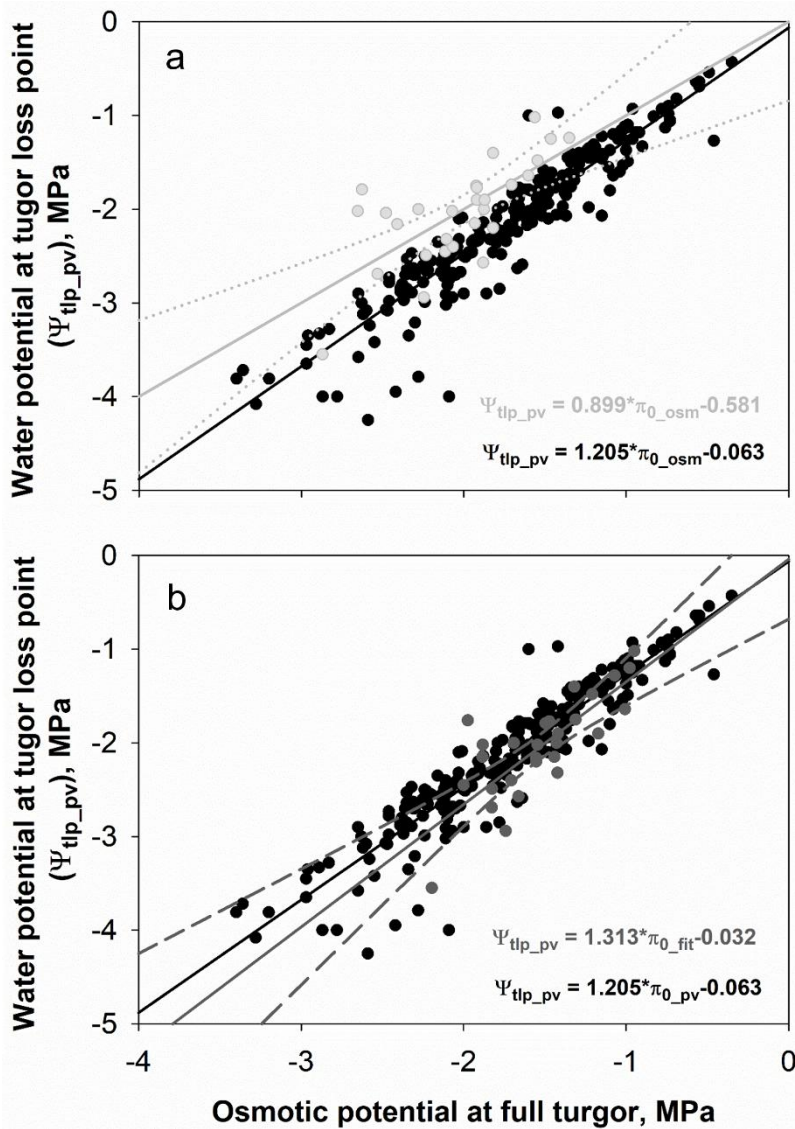


**Fig. 2** Relationship between water potential at turgor loss point measured through pv-curves ( $\Psi_{\text{tlp\_pv}}$ ) and the osmotic potential at full turgor measured with a dewpoint hygrometer ( $\pi_{0\_osm}$ , light grey circles, a), the fitted values of the MAM ( $\pi_{0\_fit}$ , dark grey circles, b) and the osmotic potential at full turgor from Bartlett et al. (2012b, black circles). Dotted light green line represents confidence intervals of the regression line calculated considering  $\pi_{0\_osm}$  (solid light grey line, a). Dashed dark grey line represents confidence intervals of the regression line calculated considering  $\pi_{0\_fit}$  (solid dark grey line, b). Solid black lines represent regression lines calculated on data from Bartlett et al. (2012b).

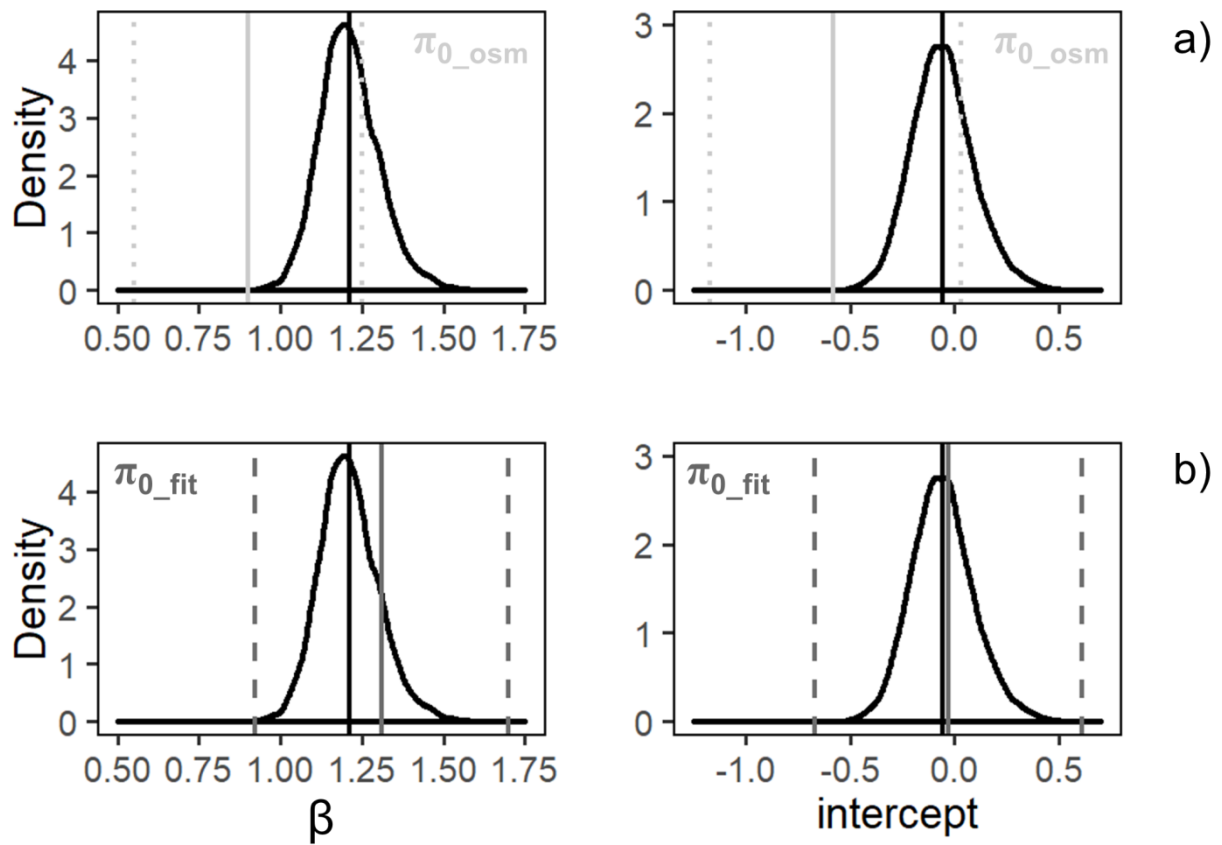


**Fig. 3** Density probability and associated mean values (black solid lines) of coefficient  $\beta$  and intercept of the model predicting  $\Psi_{tip\_pv}$  calculated on a reduced subset of data from Bartlett et al. (2012b). Solid and dotted light grey lines represent mean values and 95% C.I. of coefficient  $\beta$  and intercept calculated on the model including  $\pi_{0\_osm}$  as predictive variable (a). Solid and dashed dark grey lines represent mean values and 95% C.I. of coefficient  $\beta$  and intercept calculated on the model including  $\pi_{0\_fit}$  as predictive variable (b).

#### 4. DISCUSSION

As reported by Bartlett et al. (2012a),  $\pi_{0\_osm}$  significantly correlated with  $\pi_{0\_pv}$  (Fig. 1), but the regression line was different from the desired 1:1 relationship. A reason for this discrepancy is that osmometer-based measurements of  $\pi_0$  could be biased by errors due to sample preparation. In fact, the disruption of cell walls could cause the dissolution of cell walls solutes that could lead to more negative  $\pi_0$  values. On the other hand, symplastic fluids could be diluted by apoplastic water, leading to higher  $\pi_0$  values. In this light, testing whether this prediction could be improved is fundamental to provide a solid framework for fast and reliable  $\pi_0$  estimation. In the present study, we measured several leaf morpho-anatomical traits in order to enhance the predictive power of  $\pi_{0\_pv}$  from measurements done with an hygrometer ( $\pi_{0\_osm}$ ) on the basis of the framework proposed by Bartlett et al. (2012a).

The best model to predict  $\pi_{0\_pv}$  included  $\pi_{0\_osm}$  and LDMC, enhancing the predictive power of the model including only  $\pi_{0\_osm}$ , as  $R^2_{adj}$  was higher and AICc and MAE were lower (Tab. 1). As previously suggested by Bartlett et al. (2012a), the inclusion of LDMC in the predictive model could account for both errors associated to osmometer measurements. Higher values of LDMC are associated to greater cell wall investment, which in turn could improve the maintenance of relatively high water content, thus accounting for apoplastic dilution. On the other hand, higher LDMC could also reflect thicker cell walls or leaf with smaller but more numerous cells, thus accounting for solutes concentration enrichment derived from cell walls disruption.

In their analysis, Bartlett et al. (2012a) found that the best models to predict  $\pi_{0\_pv}$  included  $d_{leaf}$ ,  $\pi_{0\_osm}$  and their interaction, or just  $\epsilon$  and  $\pi_{0\_osm}$ . In our analysis,  $d_{leaf}$  was discarded during model selection and the model including  $\epsilon$  had less predictive power than the model including LDMC. These discrepancies could be due to multiple factors. Both studies included a limited number of species (30 in Bartlett et al. (2012a) and 27 in the present study), adapted to different environments. Most of the species in the present study are typical of Mediterranean biomes, while most of the species in Bartlett et al. (2012a) originate from temperate and tropical biomes. Consequently, drought tolerance and turgor loss point could be driven by different morpho-anatomical features in the two sets of species. Moreover, whereas minimum and maximum  $\pi_{0\_pv}$  values were nearly the same between the two datasets, the distribution of density probability of  $\pi_0$  was more skewed in Bartlett et al. (2012a)

(Fig. S1), indicating a higher density of observations in a narrower range of  $\pi_0$  values. However, a sort of consensus approach could be derived from these analyses. In both studies, the best model to predict  $\pi_{0_{pv}}$  included traits which reflect leaf carbon investment ( $d_{leaf}$ , LDMC and  $\epsilon$ ), suggesting that species that sustain higher leaf construction costs (denser and/or thicker leaves), and thus occupy the “slow-growing” space of leaf economic spectrum (Wright et al., 2004), also have higher drought resistance. The framework provided by Bartlett et al. (2012a) could allow to estimate  $\pi_0$  and  $\Psi_{t_{lp}}$  on a large number of species and samples strongly reducing the time needed for its measurement using pv-curves. The framework provided in this study further simplifies the model proposed by Bartlett et al. (2012a), as the measurement of LDMC is faster and simpler than the procedure for  $d_{leaf}$  measurement.

$\pi_0$  and  $\Psi_{t_{lp}}$  are strongly correlated with each other (Bartlett et al., 2012b) and thus, it is possible to estimate  $\Psi_{t_{lp}}$  from measurements of  $\pi_0$ . A significant linear relationship between  $\pi_0$  and  $\Psi_{t_{lp}}$  was found in the regression models run on the data provided by the authors (Tab. 2). We used parameters estimates of this model as a reference to compare regression models with  $\pi_{0_{osm}}$  or  $\pi_{0_{fit}}$  as predictive variable. The model including  $\pi_{0_{osm}}$  resulted very similar to the one obtained by Bartlett et al. (2012a):

$$\Psi_{t_{lp_{pv}}} = 0.832 \pi_{0_{osm}} - 0.631 \quad (\text{eqn 4, from Bartlett et al. 2012a})$$

$$\Psi_{t_{lp_{pv}}} = 0.899 \pi_{0_{osm}} - 0.581 \quad (\text{eqn 5})$$

However, the regression model in eqn 5 had a lower predictive power and parameters' estimates were slightly different than those calculated from the model run on data from Bartlett et al. (2012b) (Tab. 2). As shown in Fig. 2, we detected a discrepancy between the regression model considering  $\pi_{0_{osm}}$  as the predictive variable and the one calculated on data from Bartlett et al. (2012b). In particular,  $\Psi_{t_{lp}}$  values  $< -2$  MPa tended to be overestimated by eqn 2. On the contrary, the model considering  $\pi_{0_{fit}}$  as explanatory variable produced parameters' estimates much closer to those obtained from data provided in Bartlett et al. (2012b) (Fig. 2) and no discrepancy was detected.

The number of studies including  $\pi_0$  and  $\Psi_{t_{lp}}$  estimation from osmometer/hygrometer measurement of  $\pi_0$  rapidly increased in the last years (Maréchaux et al., 2015; Petruzzellis et al., 2018, 2017), and it is likely that the

350 number of species with associated  $\Psi_{\text{tlp}}$  values will increase as well. In this light, the  
351 standardization and the simplification of the framework for  $\Psi_{\text{tlp}}$  estimation is crucial to  
352 build a solid global dataset. To improve the predictive power of the estimation of  $\Psi_{\text{tlp}}$ ,  
353 we suggest measuring LDMC as well as  $\pi_{0\_osm}$  from leaves attached to the same  
354 twig or at least belonging to the same individual. To estimate  $\pi_0$  and  $\Psi_{\text{tlp}}$  we then  
355 suggest applying the following equations:

$$\pi_{0\_fit} = 0.506\pi_{0\_osm} - 0.002LDMC \text{ (expressed in mg g}^{-1}\text{)} \quad (\text{eqn 6})$$

$$\Psi_{\text{tlp\_pv}} = 1.313\pi_{0\_fit} - 0.032 \quad (\text{eqn 7})$$

358 Clearly, the inclusion of more species and  $\pi_0$  values in this type of analysis is needed  
359 to furtherly optimize the framework for  $\Psi_{\text{tlp}}$  estimation.

#### 362 CONTRIBUTIONS:

363 FP, TS and AN conceived and designed the study; FP and TS collected the data; FP,  
364 GB and AN analysed the data; FP, GB and AN wrote the manuscript, with the  
365 contribution of all authors.

#### 367 FUNDING:

368 This work is part of the project 'Functional traits as a tool to predict invasive potential  
369 by alien species in different native communities', funded by University of Trieste  
370 (Finanziamenti per la Ricerca di Ateneo 2015).

#### 372 ACKNOWLEDGMENTS:

373 We thank Roberto Alberti for help in collecting samples and Enrico Tordoni for helpful  
374 comments during data analysis.

#### 376 CONFLICT OF INTEREST:

377 The authors claim no conflict of interest.

378 REFERENCES

- 1  
2 379  
3  
4 380 Anderegg, W.R.L., 2015. Spatial and temporal variation in plant hydraulic traits and  
5 381 their relevance for climate change impacts on vegetation. *New Phytol.* 205,  
6 382 1008–1014.  
7  
8  
9 383 Anderegg, W.R.L., Flint, A., Huang, C., Flint, L., Berry, J.A., Davis, F.W., Sperry, J.S.,  
10 384 Field, C.B., 2015. Tree mortality predicted from drought-induced vascular  
11 385 damage. *Nat. Geosci.* 8, 367–371.  
12  
13  
14 386 Bartlett, M.K., Klein, T., Jansen, S., Choat, B., Sack, L., 2016. The correlations and  
15 387 sequence of plant stomatal, hydraulic, and wilting responses to drought. *P.*  
16 388 *Natl. A. Sci.* 113, 13098–13103.  
17  
18  
19 389 Bartlett, M.K., Scoffoni, C., Ardy, R., Zhang, Y., Sun, S., Cao, K., Sack, L., 2012a.  
20 390 Rapid determination of comparative drought tolerance traits: using an  
21 391 osmometer to predict turgor loss point: *Rapid assessment of leaf drought*  
22 392 *tolerance*. *Methods Ecol. Evol.* 3, 880–888.  
23  
24  
25 393 Bartlett, M.K., Scoffoni, C., Sack, L., 2012b. The determinants of leaf turgor loss point  
26 394 and prediction of drought tolerance of species and biomes: a global meta-  
27 395 analysis. *Ecol. Lett.* 15, 393–405.  
28  
29  
30 396 Blackman, C.J., 2018. Leaf turgor loss as a predictor of plant drought response  
31 397 strategies. *Tree Physiol.* 38, 655–657.  
32  
33  
34 398 Blackman, C.J., Brodribb, T.J., Jordan, G.J., 2012. Leaf hydraulic vulnerability  
35 399 influences species' bioclimatic limits in a diverse group of woody angiosperms.  
36 400 *Oecologia* 168, 1–10.  
37  
38  
39 401 Brodribb, T.J., 2017. Progressing from 'functional' to mechanistic traits. *New Phytol.*  
40 402 215, 9–11.  
41  
42  
43 403 Brodribb, T.J., Holbrook, N.M., Edwards, E.J., Gutierrez, M.V., 2003. Relations  
44 404 between stomatal closure, leaf turgor and xylem vulnerability in eight tropical  
45 405 dry forest trees. *Plant Cell Environ.* 26, 443–450.  
46  
47  
48 406 Brodribb, T.J., McAdam, S.A.M., Jordan, G.J., Martins, S.C.V., 2014. Conifer species  
49 407 adapt to low-rainfall climates by following one of two divergent pathways. *P.*  
50 408 *Natl. A. Sci.* 111, 14489–14493.  
51  
52  
53 409 Calcagno, V., 2013. glmulti: Model selection and multimodel inference made easy. R  
54 410 package version 1.0.7.  
55  
56  
57  
58  
59  
60  
61  
62  
63  
64  
65



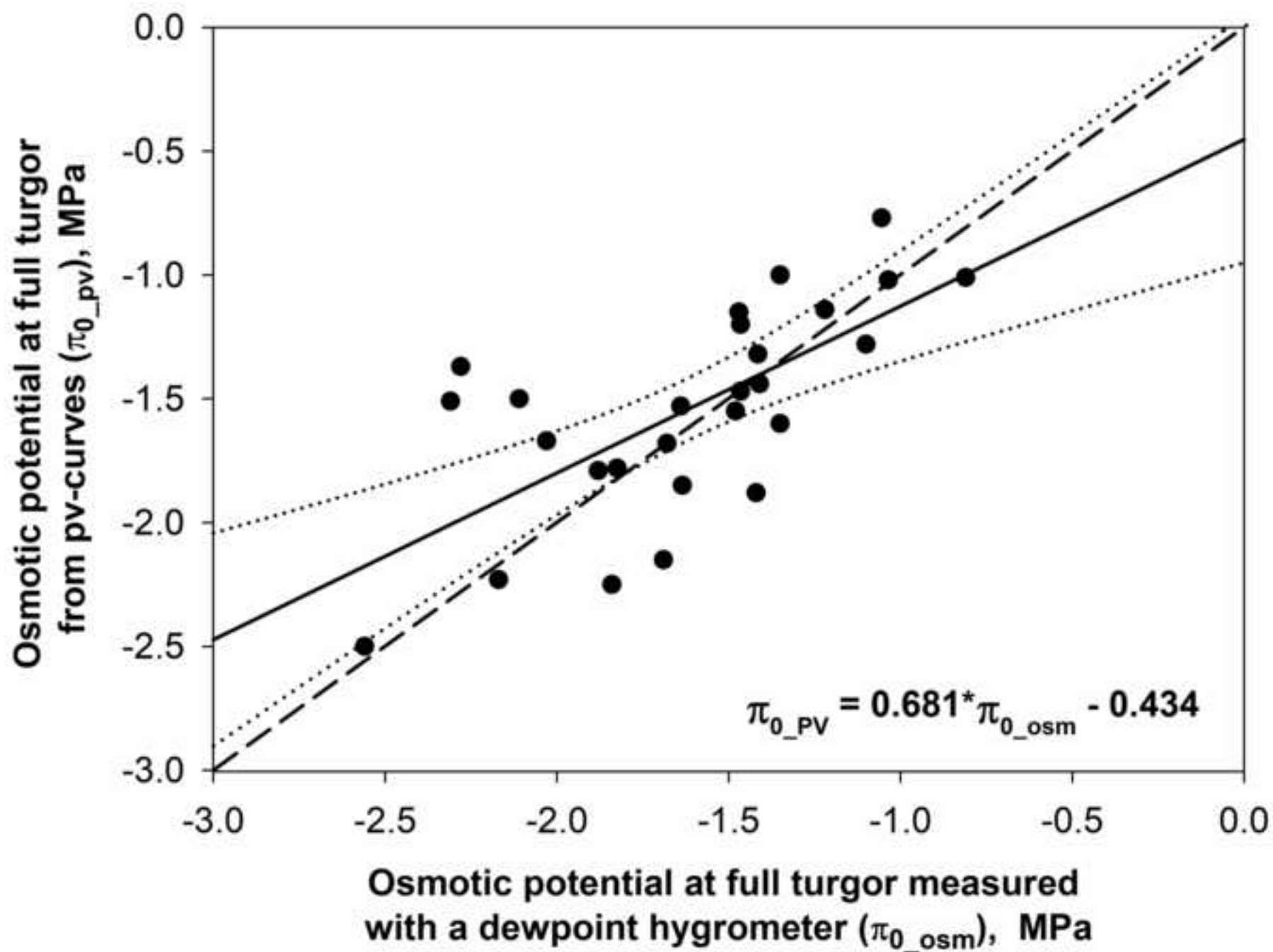
- 1 411 Choat, B., Jansen, S., Brodribb, T.J., Cochard, H., Delzon, S., Bhaskar, R., Bucci,  
2 412 S.J., Feild, T.S., Gleason, S.M., Hacke, U.G., Jacobsen, A.L., Lens, F.,  
3 413 Maherali, H., Martínez-Vilalta, J., Mayr, S., Mencuccini, M., Mitchell, P.J.,  
4 414 Nardini, A., Pittermann, J., Pratt, R.B., Sperry, J.S., Westoby, M., Wright, I.J.,  
5 415 Zanne, A.E., 2012. Global convergence in the vulnerability of forests to  
6 416 drought. *Nature* 491, 752–755.
- 7 417 Costa-Saura, J.M., Martínez-Vilalta, J., Trabucco, A., Spano, D., Mereu, S., 2016.  
8 418 Specific leaf area and hydraulic traits explain niche segregation along an  
9 419 aridity gradient in Mediterranean woody species. *Perspect. Plant Ecol.* 21, 23–  
10 420 30.
- 11 421 Fan, Z.-X., Zhang, S.-B., Hao, G.-Y., Ferry Slik, J.W., Cao, K.-F., 2012. Hydraulic  
12 422 conductivity traits predict growth rates and adult stature of 40 Asian tropical  
13 423 tree species better than wood density. *J. Ecol.* 100, 732–741.
- 14 424 Larter, M., Pfautsch, S., Domec, J.-C., Trueba, S., Nagalingum, N., Delzon, S., 2017.  
15 425 Aridity drove the evolution of extreme embolism resistance and the radiation of  
16 426 conifer genus *Callitris*. *New Phytol.* 215, 97–112.
- 17 427 Lenz, T.I., Wright, I.J., Westoby, M., 2006. Interrelations among pressure-volume  
18 428 curve traits across species and water availability gradients. *Physiol. Plantarum*  
19 429 127, 423–433. Maréchaux, I., Bartlett, M.K., Sack, L., Baraloto, C., Engel, J.,  
20 430 Joetzier, E., Chave, J., 2015. Drought tolerance as predicted by leaf water  
21 431 potential at turgor loss point varies strongly across species within an  
22 432 Amazonian forest. *Funct. Ecol.* 29, 1268–1277.
- 23 433 Nardini, A., Luglio, J., 2014. Leaf hydraulic capacity and drought vulnerability:  
24 434 possible trade-offs and correlations with climate across three major biomes.  
25 435 *Funct. Ecol.* 28, 810–818.
- 26 436 Nardini, A., Pedà, G., Rocca, N.L., 2012. Trade-offs between leaf hydraulic capacity  
27 437 and drought vulnerability: morpho-anatomical bases, carbon costs and  
28 438 ecological consequences. *New Phytol.* 196, 788–798.
- 29 439 Petruzzellis, F., Nardini, A., Savi, T., Tonet, V., Castello, M., Bacaro, G., 2018. Less  
30 440 safety for more efficiency: water relations and hydraulics of the invasive tree  
31 441 *Ailanthus altissima* (Mill.) Swingle compared with native *Fraxinus ornus* L.  
32 442 *Tree Physiol.* 39, 76–87.

443 Petruzzellis, F., Palandrani, C., Savi, T., Alberti, R., Nardini, A., Bacaro, G., 2017.  
1  
2 444 Sampling intraspecific variability in leaf functional traits: Practical suggestions  
3  
4 445 to maximize collected information. *Ecol. Evol.* 7, 11236–11245.  
5  
6 446 Savi, T., Marin, M., Luglio, J., Petruzzellis, F., Mayr, S., Nardini, A., 2016a. Leaf  
7 447 hydraulic vulnerability protects stem functionality under drought stress in  
8  
9 448 *Salvia officinalis*. *Funct. Plant. Biol.* 43, 370–379.  
10  
11 449 Savi, T., Casolo, V., Luglio, J., Bertuzzi, S., Trifilo', P., Lo Gullo, M.A., Nardini, A.,  
12  
13 450 2016b. Species-specific reversal of stem xylem embolism after a prolonged  
14  
15 451 drought correlates to endpoint concentration of soluble sugars. *Plant Physiol.*  
16  
17 452 *Bioch.* 106, 198–207.  
18  
19 453 Savi, T., Dal Borgo, A., Love, V.L., Andri, S., Tretiach, M., Nardini, A., 2016c.  
20 454 Drought versus heat: What's the major constraint on Mediterranean green roof  
21  
22 455 plants? *Sci. Total Environ.* 566–567, 753–760.  
23  
24 456 Savi, T., Love V.L., Borgo A.D., Martellos S., Nardini A., 2017. Morpho-anatomical  
25  
26 457 and physiological traits in saplings of drought-tolerant Mediterranean woody  
27  
28 458 species. *Trees* 31,356 1137–1148.  
29  
30 459 Schneider, C.A., Rasband, W.S., Eliceiri, K.W., 2012. NIH Image to ImageJ: 25 years  
31 460 of image analysis. *Nat. Methods* 9, 671–675.  
32  
33 461 Tognetti, R., Raschi, A., Jones, M.B., 2000. Seasonal patterns of tissue water  
34  
35 462 relations in three Mediterranean shrubs co-occurring at a natural CO<sub>2</sub> spring.  
36  
37 463 *Plant Cell Environ.* 23, 1341–1351.  
38  
39 464 Trifiló, P., Raimondo, F., Savi, T., Lo Gullo, M.A., Nardini, A., 2016. The contribution  
40 465 of vascular and extra-vascular water pathways to drought-induced decline of  
41  
42 466 leaf hydraulic conductance. *J. Exp. Bot.* 67, 5029–5039.  
43  
44 467 Tyree, M.T., Hammel, H.T., 1972. The Measurement of the Turgor Pressure and the  
45  
46 468 Water Relations of Plants by the Pressure-bomb Technique. *J. Exp. Bot.* 23,  
47  
48 469 267–282.  
49  
50 470 Violle, C., Navas, M.-L., Vile, D., Kazakou, E., Fortunel, C., Hummel, I., Garnier, E.,  
51 471 2007. Let the concept of trait be functional! *Oikos* 116, 882–892.  
52  
53 472 Wright, I.J., Reich, P.B., Westoby, M., Ackerly, D.D., Baruch, Z., Bongers, F.,  
54  
55 473 Cavender-Bares, J., Chapin, T., Cornelissen, J.H., Diemer, M., 2004. The  
56  
57 474 worldwide leaf economics spectrum. *Nature* 428, 821–827.  
58  
59  
60  
61  
62  
63  
64  
65

475 Zhu, S.-D., Chen, Y.-J., Ye, Q., He, P.-C., Liu, H., Li, R.-H., Fu, P.-L., Jiang, G.-F.,  
1  
2 476 Cao, K.-F., 2018. Leaf turgor loss point is correlated with drought tolerance  
3  
4 477 and leaf carbon economics traits. *Tree Physiol.* 38, 658–663.  
5  
6  
7  
8  
9  
10  
11  
12  
13  
14  
15  
16  
17  
18  
19  
20  
21  
22  
23  
24  
25  
26  
27  
28  
29  
30  
31  
32  
33  
34  
35  
36  
37  
38  
39  
40  
41  
42  
43  
44  
45  
46  
47  
48  
49  
50  
51  
52  
53  
54  
55  
56  
57  
58  
59  
60  
61  
62  
63  
64  
65

**CONTRIBUTIONS:**

FP, TS and AN conceived and designed the study; FP and TS collected the data; FP, GB and AN analysed the data; FP, GB and AN wrote the manuscript, with the contribution of all authors.



Figure

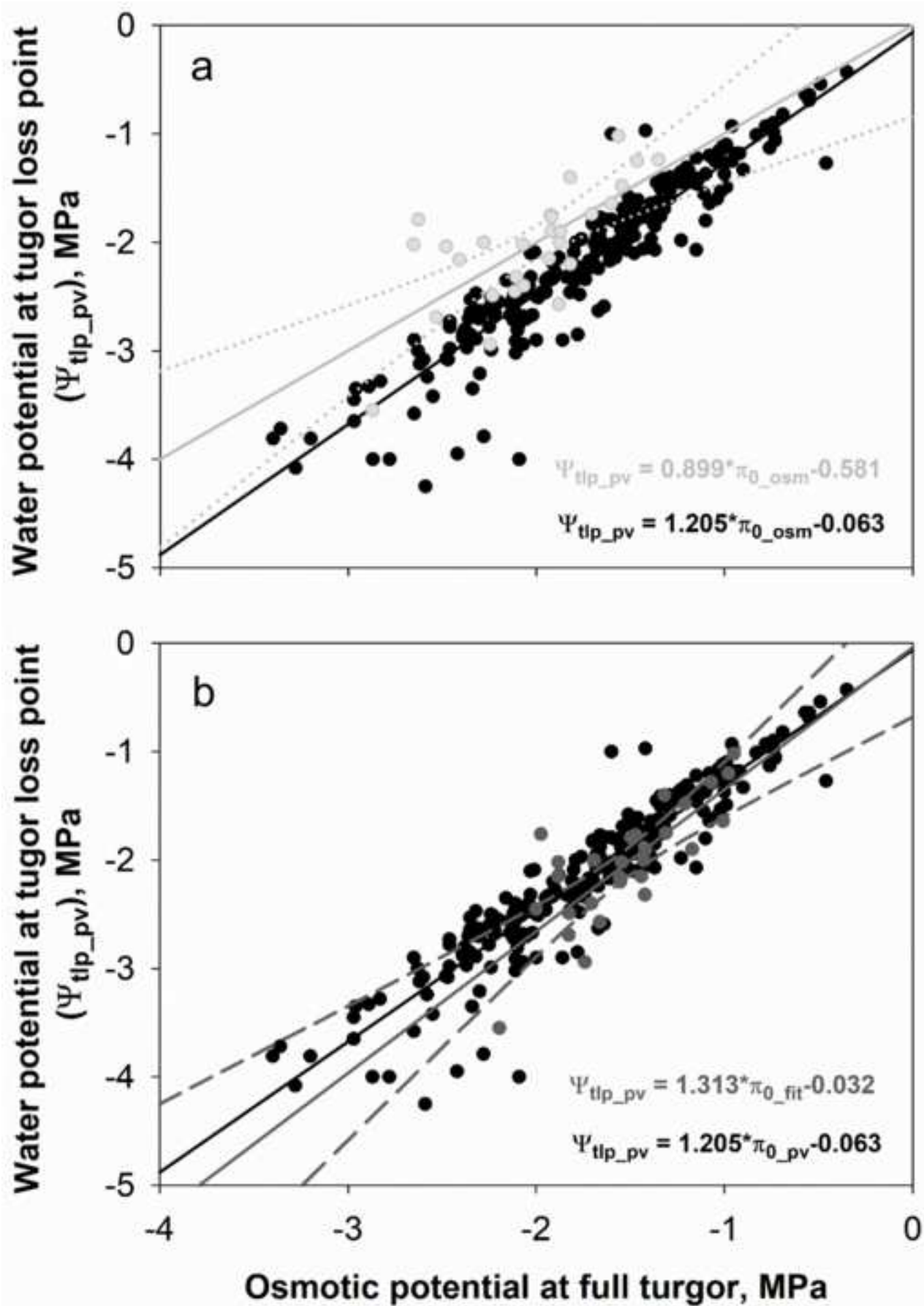
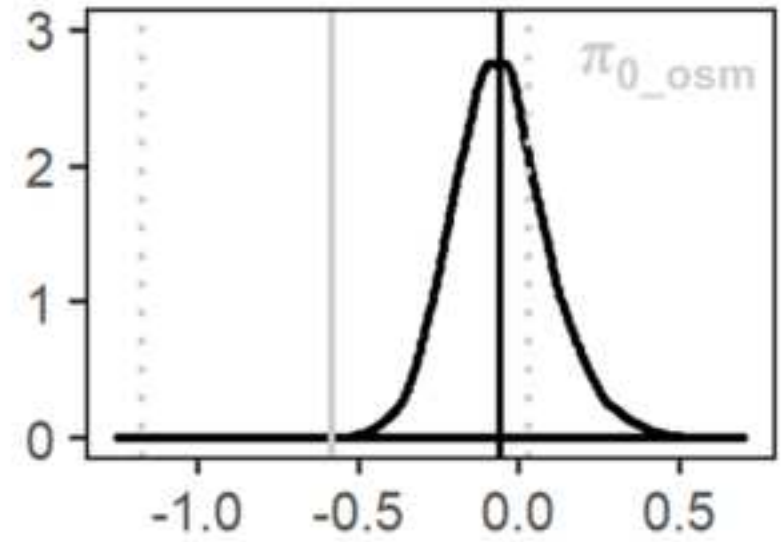
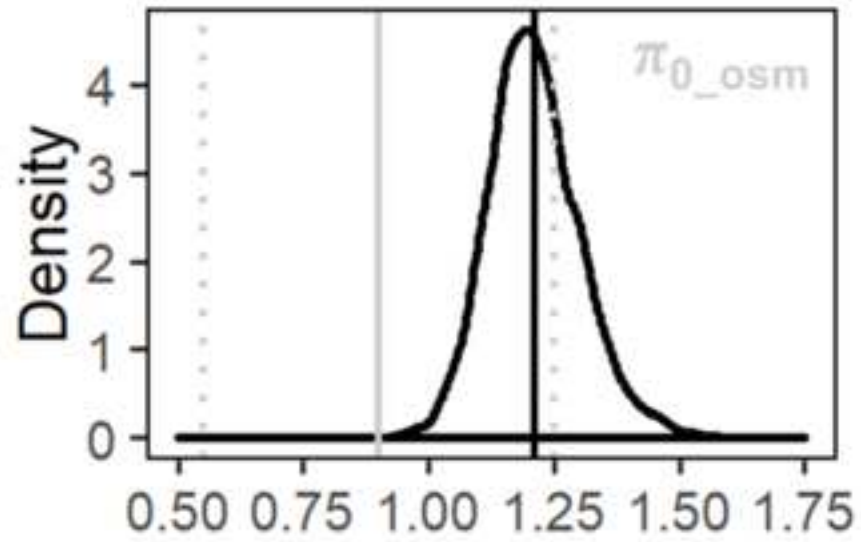
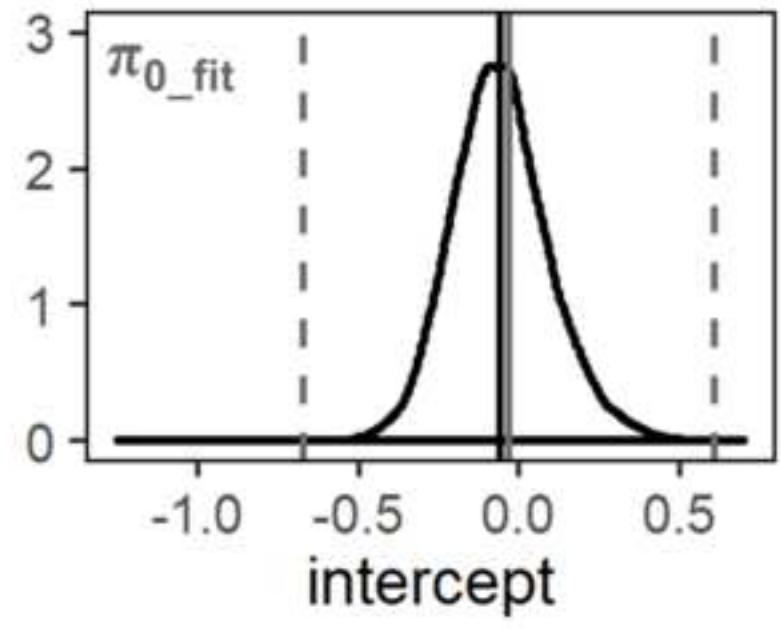
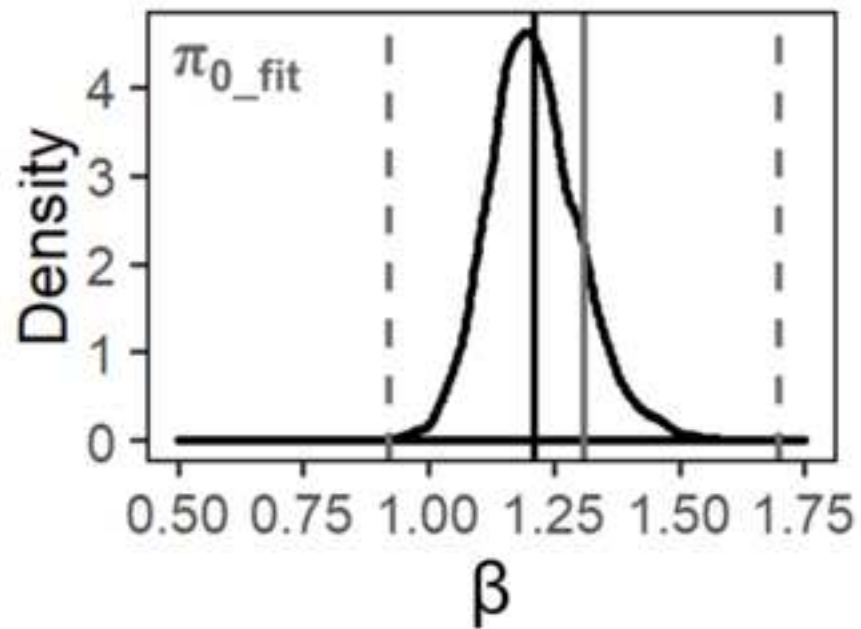
[Click here to download high resolution image](#)

Figure  
[Click here to download high resolution image](#)

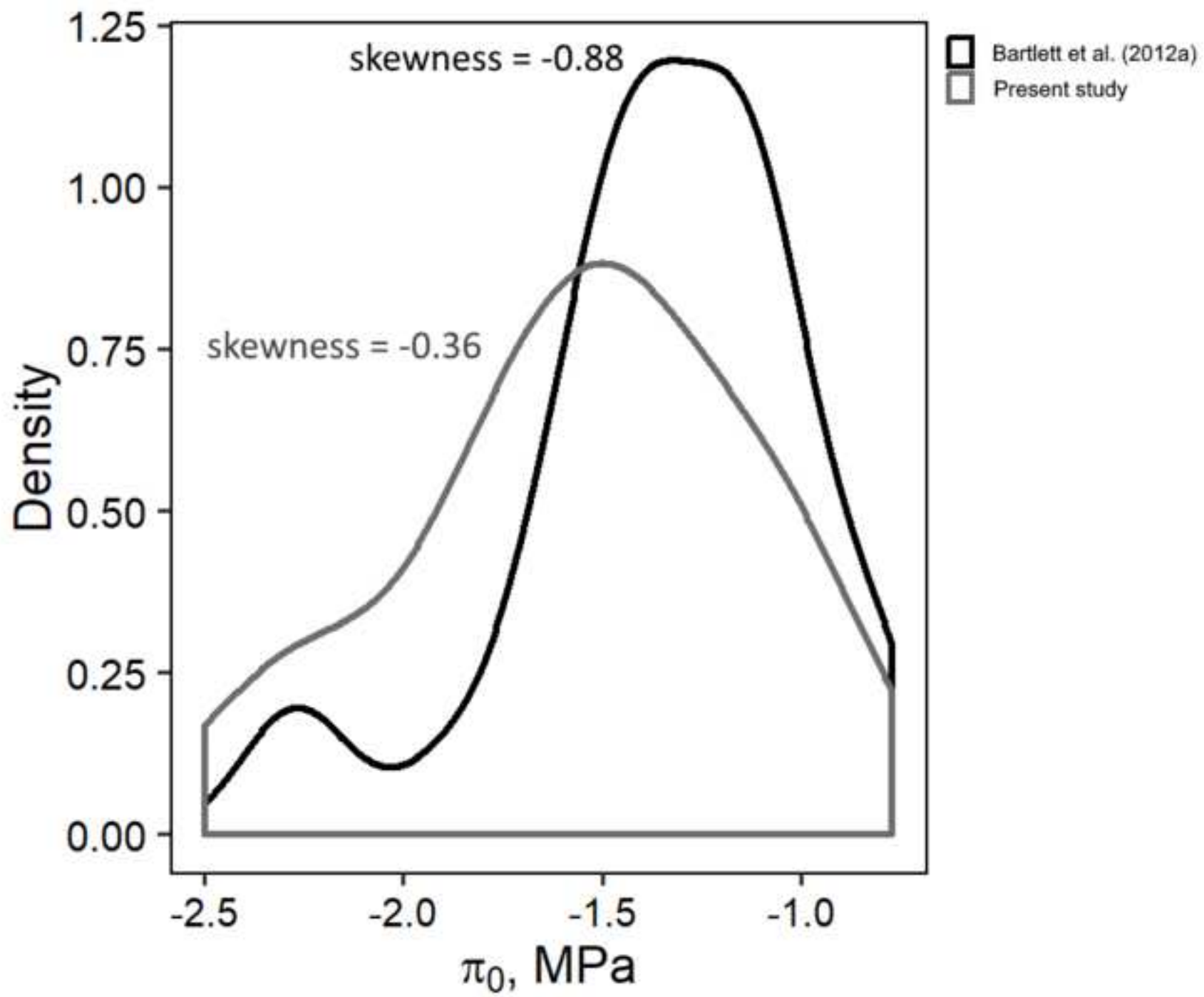


a)



b)

Figure  
[Click here to download high resolution image](#)





**Supplementary material**

[Click here to download Supplementary material: TabS1.xlsx](#)

**Supplementary material**

[Click here to download Supplementary material: Supplementary\\_PPB\\_rev.docx](#)